Light quark masses with overlap fermions in quenched QCD

L. Giusti, C. Hoelbling, and C. Rebbi

Department of Physics, Boston University, 590 Commonwealth Avenue, Boston, Massachusetts 02215

We present the results of a computation of the sum of the strange and average up-down quark masses with overlap fermions in the quenched approximation. Since the overlap regularization preserves chiral symmetry at finite cutoff and volume, no additive quark mass renormalization is required and the results are $\mathcal{O}(a)$ improved. Our simulations are performed at $\beta = 6.0$ and volume $V = 16^3 \times 32$, which correspond to a lattice cutoff of ~ 2 GeV and to an extension of ~ 1.4 fm. The logarithmically divergent renormalization constant has been computed nonperturbatively in the RI/MOM scheme. By using the K-meson mass as experimental input, we obtain $(m_s + \hat{m})^{\mathrm{RI}}(2 \ \mathrm{GeV}) = 120(7)(21)$ MeV, which corresponds to $m_s^{\overline{\mathrm{MS}}}(2 \ \mathrm{GeV}) = 102(6)(18)$ MeV if continuum perturbation theory and χPT are used. By using the Gell-Mann–Oakes–Renner relation we also obtain $\langle \bar{\psi}\psi \rangle^{\overline{\mathrm{MS}}}(2 \ \mathrm{GeV})/N_f = -0.0190(11)(33) \ \mathrm{GeV}^3 = -[267(5)(15) \ \mathrm{MeV}]^3$, where the errors are statistical and systematic respectively.

I. INTRODUCTION

Quark masses are fundamental parameters of the standard model which cannot be measured directly by experiment, since quarks are confined into hadrons. If defined as effective couplings in the Lagrangian, their values can be determined by comparing a theoretical calculation of a given physical quantity (sensitive to quark masses) with the corresponding experimental value. As a consequence quark masses depend on the renormalization scheme and scale, as well as on the fundamental action.

At present the most precise values of light-quark mass ratios (which are scheme and scale independent for mass independent renormalization schemes) are extracted by comparing K- and π-meson mass ratios with predictions from chiral perturbation theory (χPT) [1]. A detailed analysis gives [2]

$$\frac{m_u}{m_d} = 0.553 \pm 0.043, \qquad \frac{m_s}{\hat{m}} = 24.4 \pm 1.5 \qquad (1)$$

where $\hat{m} = (m_u + m_d)/2$. The absolute scale cannot be fixed by χPT. It can be determined by comparing non-perturbative lattice QCD computations [3–15] or phenomenological estimates [16,17] with experimental results.

In the last few years much effort has been devoted within the lattice community to obtain a precise determination of the light quark masses in the quenched approximation. Major improvements came with the use of nonperturbative (NP) renormalization techniques for renormalizing the bare quark masses and with the implementation of $\mathcal{O}(a)$ improved actions and operators [7,9,10,14] (for a recent review see [18]). First results from unquenched simulations have also been reported [8,15,18].

In this paper we present the results of the first fully non-perturbative computation of $(m_s + \hat{m})$ with overlap fermions. In this fermionic regularization, flavor and chiral symmetries are preserved at finite lattice spacing and finite volume. As a consequence no additive quark mass renormalization is re-

quired and no parameters have to be fine tuned in order to compute $\mathcal{O}(a)$ improved masses and matrix elements. To avoid uncertainties due to lattice perturbation theory, we compute the logarithmic divergent renormalization constant non-perturbatively in the RI/MOM (momentum subtraction) scheme [19]. By comparing the experimental K-meson mass with the value obtained in our simulations and after a careful analysis of the systematic uncertainties we find as our main result

$$(m_s + \hat{m})^{\mathrm{RI}}(2 \ \mathrm{GeV}) = 120 \pm 7 \pm 21 \ \mathrm{MeV}. \qquad (2)$$

This value corresponds to

$$m_s^{\overline{\mathrm{MS}}}(2 \ \mathrm{GeV}) = 102 \pm 6 \pm 18 \ \mathrm{MeV} \qquad (3)$$

if next-to-next-to-leading order (NNLO) continuum perturbative results and Eq. (1) are used.

We also report results for the chiral condensate $\langle \bar{\psi}\psi \rangle$ which we compute from the Gell-Mann–Oakes–Renner (GMOR) relation. Our best determination is

$$\frac{1}{N_f} \langle \bar{\psi}\psi \rangle^{\mathrm{RI}}(2 \ \mathrm{GeV}) = -0.0167 \pm 0.0010 \pm 0.0029 \ \mathrm{GeV}^3 \qquad (4)$$

which corresponds to

$$\frac{1}{N_f} \langle \bar{\psi}\psi \rangle^{\overline{\mathrm{MS}}}(2 \ \mathrm{GeV}) = -0.0190 \pm 0.0011 \pm 0.0033 \ \mathrm{GeV}^3$$

$$= -[267 \pm 5 \pm 15 \ \mathrm{MeV}]^3. \qquad (5)$$

We have also computed the chiral condensate directly. Even if it requires a severe chiral extrapolation, the direct determination gives results consistent with Eqs. (4) and (5).

The first error in Eqs. (2)–(5) represents the statistical error, obtained with the jackknife method. The second error represents our estimate of systematic effects. It should be noted that, while the systematic error due to quenching alone (defined as the quenching error in the limit of zero lattice

spacing and infinite volume) should be the same in all fermionic regularizations, discretization errors do depend on the fermionic lattice action and are likely to be smaller in the overlap formulation because of its good chirality properties. The very good agreement of our results with the current lattice world averages [18] provides further confirmation that the overlap formulation is a suitable regularization for large-scale phenomenological computations.

This paper is organized as follows: in Sec. II we set our notation and define the renormalized quark masses and chiral condensate in the overlap regularization; in Sec. III we give details about the simulation and some of the results for the meson masses and matrix elements; in Sec. IV we present our main results and discuss their systematic errors; Sec. V is devoted to our concluding remarks.

II. QUARK MASSES AND CHIRAL CONDENSATE WITH THE OVERLAP ACTION

The QCD lattice action in the overlap regularization reads [20]

$$S = \frac{6}{g_0^2} \sum_P \left[1 - \frac{1}{6} \mathrm{Tr}[U_P + U_P^\dagger] \right] + \bar{\psi} \left[\left(1 - \frac{1}{2\rho} aM \right) D + M \right] \psi \tag{6}$$

where, in standard notation, U_P is the Wilson plaquette, $g_0 = \sqrt{6/\beta}$ is the bare coupling constant, ψ and $\bar{\psi}$ carry implicit color, spin and flavor indices, and M is a diagonal matrix of bare masses $(m_1, m_2, \dots)$ in flavor space. D is the Neuberger-Dirac operator defined as

$$D = \frac{\rho}{a}(1 + V) = \frac{\rho}{a} \left(1 + X \frac{1}{\sqrt{X^\dagger X}} \right)$$

$$X = D_W - \frac{1}{a}\rho \tag{7}$$

where

$$D_W = \frac{1}{2} \gamma_\mu (\nabla_\mu + \nabla_\mu^*) - \frac{r}{2} a \nabla_\mu^* \nabla_\mu \tag{8}$$

is the Wilson-Dirac operator, $0 < r \leq 1$ and $0 < \rho < 2r$. In our calculations we used $r = 1$. ∇_μ and ∇_μ^* in Eq. (8) are the forward and backward lattice covariant derivatives, defined by

$$\nabla_\mu \psi(x) = \frac{1}{a} [U_\mu(x)\psi(x + a\hat{\mu}) - \psi(x)], \tag{9}$$

$$\nabla_\mu^* \psi(x) = \frac{1}{a} [\psi(x) - U_\mu^\dagger(x - a\hat{\mu})\psi(x - a\hat{\mu})] \tag{10}$$

where $U_\mu(x)$ are the lattice gauge links. The fermionic operator of the overlap action satisfies the Ginsparg-Wilson relation [21]

$$\gamma_5 D + D \gamma_5 = \frac{a}{\rho} D \gamma_5 D, \tag{11}$$

which implies an exact continuous symmetry of the action in the massless limit [22]. This symmetry may be interpreted as a lattice form of chiral invariance at finite cutoff

$$\delta\psi = \hat{\gamma}_5 \psi, \quad \delta\bar{\psi} = \bar{\psi}\gamma_5 \tag{12}$$

where $\hat{\gamma}_5$ is defined as

$$\hat{\gamma}_5 = \gamma_5 \left(1 - \frac{a}{\rho} D \right) \tag{13}$$

and satisfies

$$\hat{\gamma}_5^\dagger = \hat{\gamma}_5, \quad \hat{\gamma}_5^2 = 1. \tag{14}$$

The anomaly is recovered from the variation of the measure under the rotations in Eq. (12) [22,23].

The invariance of the action under non-singlet chiral transformations, defined including a flavor group generator in Eq. (12), forbids mixing among operators of different chirality [24] and therefore:

No additive quark mass renormalization is required. The quark mass which enters the vector and axial Ward identities is the bare parameter $m(a)$ in the action of Eq. (6).

Masses and matrix elements are affected only by $\mathcal{O}(a^2)$ discretization errors. No fine tuned parameters are required to remove $\mathcal{O}(a)$ effects.

The chiral condensate does not require subtractions of power divergent terms (in the chiral limit).

The renormalized quark mass is defined as

$$\bar{m}(\mu) = \lim_{a \to 0} Z_m(a\mu) m(a) \tag{15}$$

where $Z_m(a\mu)$ is a logarithmically divergent renormalization constant which has to be fixed, for a given scale μ, in a given renormalization scheme. It is worth noting that even if $m(a)$ is the bare parameter which enters the fundamental action in Eq. (6), its relation to a given experimental result is fixed by a non-perturbative lattice QCD calculation and therefore its value is determined up to $\mathcal{O}(a^2)$ terms only.

The bare chiral condensate is defined as

$$\chi(a) \equiv \lim_{m \to 0} \frac{1}{N_f} \left\langle \bar{\psi}(0) \left[\left(1 - \frac{a}{2\rho} D \right) \psi \right](0) \right\rangle \tag{16}$$

where m is a common mass given to the light quarks. It satisfies the integrated non-singlet chiral Ward identity

$$\frac{1}{N_f} \left\langle \bar{\psi}(0) \left[\left(1 - \frac{a}{2\rho} D \right) \psi \right](0) \right\rangle = m \sum_x \langle P(x) P^c(0) \rangle \tag{17}$$

where

$$P(x) = \bar{\psi}_1(x) \gamma_5 \left[\left(1 - \frac{a}{2\rho} D \right) \psi_2 \right](x) \tag{18}$$

$$P^c(x) = \bar\psi_2(x)\gamma_5\left[\left(1 - \frac{a}{2\rho}D\right)\psi_1\right](x) \qquad (19)$$

correspond to the non-singlet pseudoscalar density with degenerate quarks ($m_1 = m_2$) and its conjugate. For non-zero mass the chiral condensate is still divergent and it behaves as

$$\frac{1}{N_f}\left\langle \bar\psi(0)\left[\left(1 - \frac{a}{2\rho}D\right)\psi\right](0)\right\rangle = \chi(a) + \beta_\chi \frac{m(a)}{a^2}, \qquad (20)$$

where we have taken into account that chiral symmetry forces the coefficient of the linear divergence to be zero.

By writing the correlation function $\langle P(x)P^c(0)\rangle$ as a time-ordered product and by inserting a complete set of states in standard fashion we can also write

$$\chi(a) = -\lim_{m\to 0}\frac{m}{M_P^2}|\langle 0|P|P\rangle|^2, \qquad (21)$$

where M_P is the mass of the pseudoscalar state $|P\rangle$. If we use

$$2m|\langle 0|P|\pi\rangle| = f_P M_P^2 \qquad (22)$$

where f_P is the corresponding pseudoscalar decay constant, we arrive to the familiar GMOR relation

$$\chi(a) = -\lim_{m\to 0}\frac{f_P^2 M_P^2}{4m}. \qquad (23)$$

The renormalized chiral condensate is defined as

$$\frac{1}{N_f}\langle\bar\psi\psi\rangle(\mu) = \lim_{a\to 0}Z_S(a\mu)\chi(a) \qquad (24)$$

where $Z_S(\mu a)$ can be chosen to be the renormalization constant of the corresponding non-singlet scalar density which, thanks to the flavor symmetry, satisfies $Z_S(\mu a) = 1/Z_m(\mu a)$. In principle $Z_S(\mu a)$ can be computed in perturbation theory [25,26], but uncertainties due to higher order terms can be avoided using non-perturbative renormalization procedures [19,27,12]. The implementation of the RI/MOM technique [19] is straightforward in the overlap regularization, and it allows one to compute $\mathcal{O}(a)$ improved renormalization constants for generic composite operators. In the following we will use the numerical value of $Z_S^{\mathrm{RI}}(\mu a)$ we have obtained in Ref. [28] (for an alternative approach see Ref. [29]).

III. NUMERICAL DETAILS

We performed our simulation in quenched QCD with $\beta = 6.0$ and $V = 16^3 \times 32$. We used a sample of 54 gauge configurations, generated with the standard Wilson gluonic action of Eq. (6), which we retrieved from the repository at the "Gauge Connection" [30]. We computed overlap propagators from a local source for bare quark masses $ma = 0.040, 0.055, 0.070, 0.085, 0.100$ and $\rho = 1.4$ (and, as already mentioned, $r = 1.0$). For the calculation of the propagators,

we used an optimal rational approximation to the sign of the Hermitian Wilson operator, as proposed in Refs. [31,32], after explicit evaluation of the contributions from the lowest eigenvectors of $X^\dagger X$, and nested multi-conjugate gradient inversions. Details of the numerical implementation will be presented in Ref. [28]. From the propagators, we computed in the standard manner the two-points correlation functions[1]

$$G_{SS}(t) = \sum_x \langle S(x,t)S^c(0,0)\rangle \qquad (25)$$

$$G_{PP}(t) = \sum_x \langle P(x,t)P^c(0,0)\rangle \qquad (26)$$

$$G_{\nabla AP}(t) = \sum_x \langle \bar\nabla_0 A_0(x,t)P^c(0,0)\rangle \qquad (27)$$

where $P(x,t)$ and $P^c(x,t)$ have been defined in Eqs. (18) and (19),

$$S(x) = \bar\psi_1(x)\left[\left(1 - \frac{a}{2\rho}D\right)\psi_2\right](x) \qquad (28)$$

$$A_\mu(x) = \bar\psi_1(x)\gamma_\mu\gamma_5\left[\left(1 - \frac{a}{2\rho}D\right)\psi_2\right](x), \qquad (29)$$

$S^c(x)$ is defined analogously to Eq. (19) and $\bar\nabla_0$ denotes the symmetric lattice derivative in the time direction. To improve statistics $G_{SS}(t)$ and $G_{PP}(t)$ have been symmetrized around $t = T/2$ ($T = N_t = 32$). We estimated the errors by a jackknife procedure, blocking the data in groups of three configurations, and we checked that blocking in groups of different size did not produce relevant changes in the error estimates. In the first plot of Fig. 1 we show the ratio

$$\rho(t) \equiv \frac{G_{\nabla AP}(t)}{G_{PP}(t)} \qquad (30)$$

as a function of t for all simulated masses. Once ρ has been fitted to a constant in the time interval $t_1 - t_2 = 5 - 27$, a quadratic fit of the results

$$(a\rho) = \mathcal{A}_\rho + \mathcal{B}_\rho(am) + \mathcal{C}_\rho(am)^2 \qquad (31)$$

gives[2] (see the second plot in Fig. 1),

$$\mathcal{A}_\rho = -0.00002(7) \quad \mathcal{B}_\rho = 1.286(3) \quad \mathcal{C}_\rho = 0.277(12) \qquad (32)$$

where the quoted errors are statistical only. Note that the intercept is compatible with zero. This should not come as a

---

[1]Analogous correlation functions have been computed by the authors of Ref. [33]. A direct comparison with our results is not possible because we used different simulations parameters.

[2]From the coefficient $\mathcal{B}_\rho$ one can derive the value of the renormalization constant Z_A of the "local" axial current. A detailed analysis will be presented in Ref. [28].
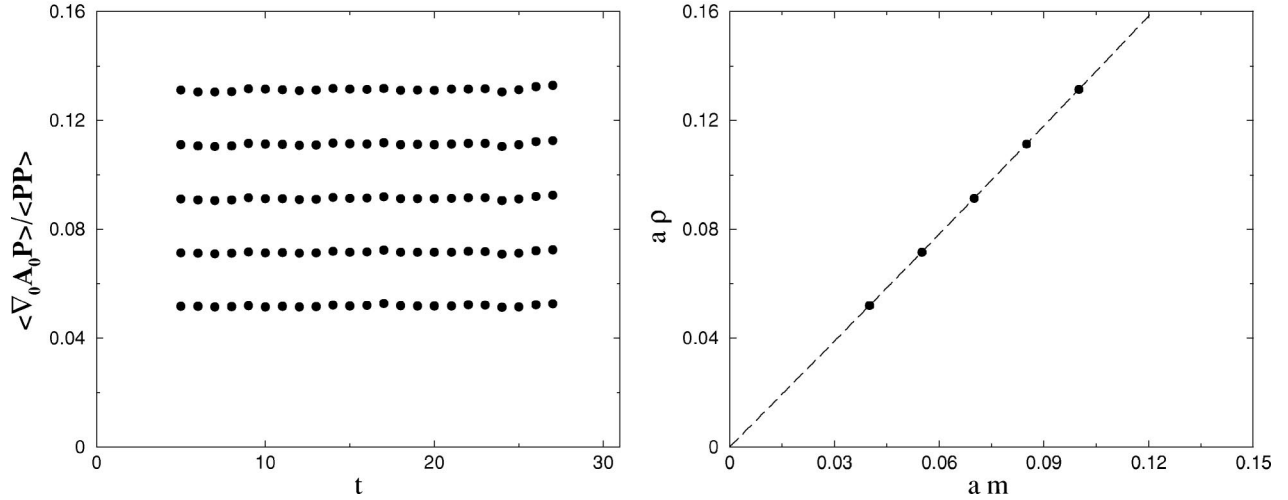
FIG. 1. Left: $G_{\nabla AP}/G_{PP}$ vs. t for all masses which have been simulated. Right: $(a\rho)$, obtained by fitting the data in the plot at left, as a function of the bare quark mass. The dashed line represents the result of a quadratic fit (see text).

surprise since, even if $A_\mu(x)$ is not the conserved current, it has the correct behavior under global non-singlet chiral transformations.

In the quenched approximation the contribution of exact chiral zero modes of the Neuberger-Dirac operator is not suppressed by the fermionic determinant. In some correlation functions, this can give rise to large quenched artifacts for small masses. For example it is easy to show that $G_{PP}(t)$ receives from the unsuppressed zero modes contributions proportional to $1/m^2$ and $1/m$, which should vanish in the infinite volume limit, but can be quite sizable for finite volume. A clever way to avoid such artifacts has been proposed by the authors of Ref. [34], who noticed that the zero modes, because of their chirality properties, contribute equally to the G_{PP} and G_{SS} correlation functions, so that their contributions cancel in the difference

$$G_{S-P}(t) = G_{PP}(t) - G_{SS}(t) \tag{33}$$

which can also be used to extract the pseudoscalar meson mass and decay constant, since the contributions from the heavier scalar mesons fall off faster. The drawback is, of course, that the plateau in the effective mass and, correspondingly, the range that can be used for the cosh fit become shorter. Nevertheless we found the plateau in the G_{S-P}

to be long enough to permit a meaningful fit. We fitted $G_{S-P}(t)$ to a single particle propagator with a cosh dependence on t,

$$G_{S-P}(t) = \frac{Z_{S-P}}{aM_P} \exp\left(-\frac{1}{2}aM_P T\right) \cosh\left[aM_P\left(\frac{T}{2}-t\right)\right] \tag{34}$$

in the time interval $t_1-t_2 = 12-16$. The lower limit was fixed at the point where we found stabilization of the effective meson masses. The results of the fits are also given in Table I and an example of the effective meson mass from $G_{S-P}(t)$ is shown in first plot of Fig. 2. We also performed a two cosh fit of $G_{S-P}(t)$ finding consistent results.

We have also fitted the correlation functions $G_{PP}(t)$ to a single particle propagator with a cosh dependence on t, as in Eq. (34), in the time interval $t_1-t_2 = 10-16$. As before the lower limit is fixed as the point at which the values of the effective meson masses become stable. We report our results in Table I and in the second plot of Fig. 2 we give an example of the effective meson mass as extracted from $G_{PP}(t)$.

We illustrate in Fig. 3 the values for $(aM_P)^2$, obtained from $G_{S-P}(t)$ and $G_{PP}(t)$, as a function of the bare quark mass am. In both cases a linear behavior

TABLE I. Mesons masses and matrix elements for all the bare quark masses considered in the simulations, as obtained from $G_{PP}(t)$ and $G_{S-P}(t)$.

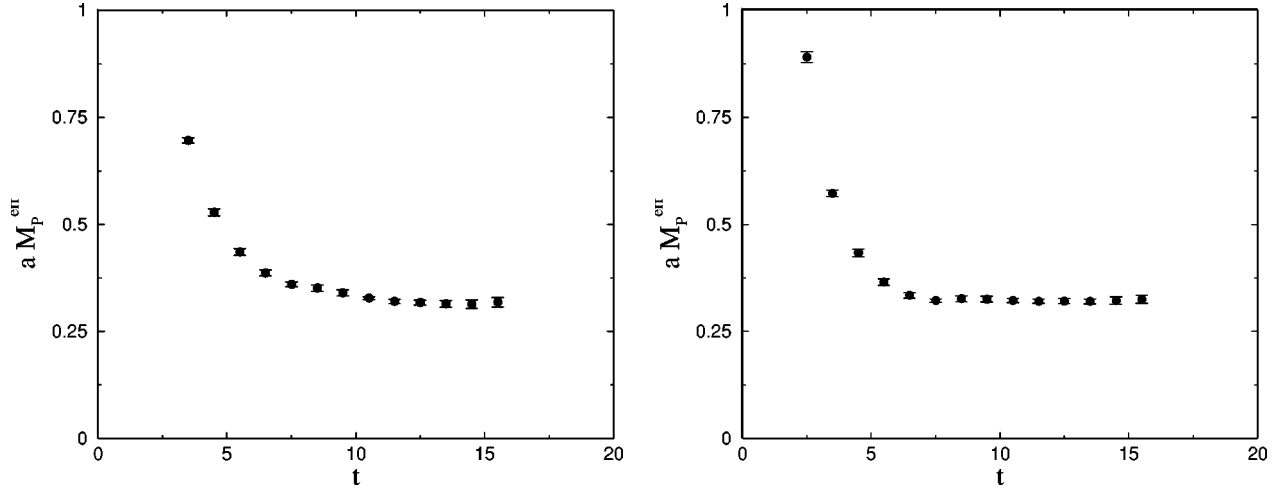| am	G_{S-P}			G_{PP}		
	Z_{S-P}	aM_P	af_P	Z_{PP}	aM_P	af_P
0.100	0.0040(4)	0.379(6)	0.089(2)	0.0042(3)	0.382(3)	0.089(2)
0.085	0.0036(4)	0.348(6)	0.085(2)	0.0039(3)	0.352(4)	0.085(2)
0.070	0.0033(4)	0.315(7)	0.081(2)	0.0036(3)	0.321(4)	0.081(2)
0.055	0.0030(5)	0.280(9)	0.076(2)	0.0034(3)	0.287(5)	0.077(2)
0.040	0.0026(5)	0.239(11)	0.071(2)	0.0032(4)	0.250(7)	0.073(2)

FIG. 2. Left: A representative example ($am=0.070$) of the effective mass from $G_{S-P}(t)$. Right: as at left but from $G_{PP}(t)$.

$$(aM_P)^2 = \mathcal{A}_{M_P} + \mathcal{B}_{M_P}(am), \qquad (35)$$

fits very well the data with

$$\mathcal{A}_{M_P} = -0.0005(68) \quad \mathcal{B}_{M_P} = 1.43(7) \qquad (36)$$

for the masses obtained from $G_{S-P}(t)$ and

$$\mathcal{A}_{M_P} = 0.006(4) \quad \mathcal{B}_{M_P} = 1.39(3) \qquad (37)$$

for those obtained from $G_{PP}(t)$. We see that the parameters of the two fits are compatible and that both intercepts vanish within statistical errors. In particular, one does not notice any sign of the singular contributions from zero modes in the masses obtained from the pseudoscalar correlation functions. These are expected to show up at some point, but one would probably need much higher statistical accuracy and lower values of m to bring them into evidence.

Contrary to the pseudoscalar masses, the results for the matrix elements, parametrized as in Eq. (34) by the factors Z_{S-P} and Z_{PP} for $G_{S-P}(t)$ and $G_{PP}(t)$, respectively, show more significant differences. In Fig. 4 we reproduce the re-sults we obtained for Z_{S-P} and Z_{PP} respectively. We see that, while Z_{S-P} exhibits a linear behavior as function of am, the graph for Z_{PP} shows a clear indication of curvature. Linear fits of the form

$$Z_i = \mathcal{A}_i + \mathcal{B}_i(am) \qquad (38)$$

give

$$\mathcal{A}_{S-P} = 0.0016(7) \quad \mathcal{B}_{S-P} = 0.024(6) \qquad (39)$$

$$\mathcal{A}_{PP} = 0.0025(4) \quad \mathcal{B}_{PP} = 0.016(3). \qquad (40)$$

Within the quite large statistical errors, the intercept and the slope obtained from $G_{S-P}(t)$ are still compatible with those derived from $G_{PP}(t)$. However the central values are quite different. If we interpret the curvature in the graph of Z_{PP} as due to pole terms from the zero modes and try a simple fit of the form

$$Z_{PP} = \mathcal{A}_{PP} + \mathcal{B}_{PP}(am) + \frac{\mathcal{D}_{PP}}{am}, \qquad (41)$$
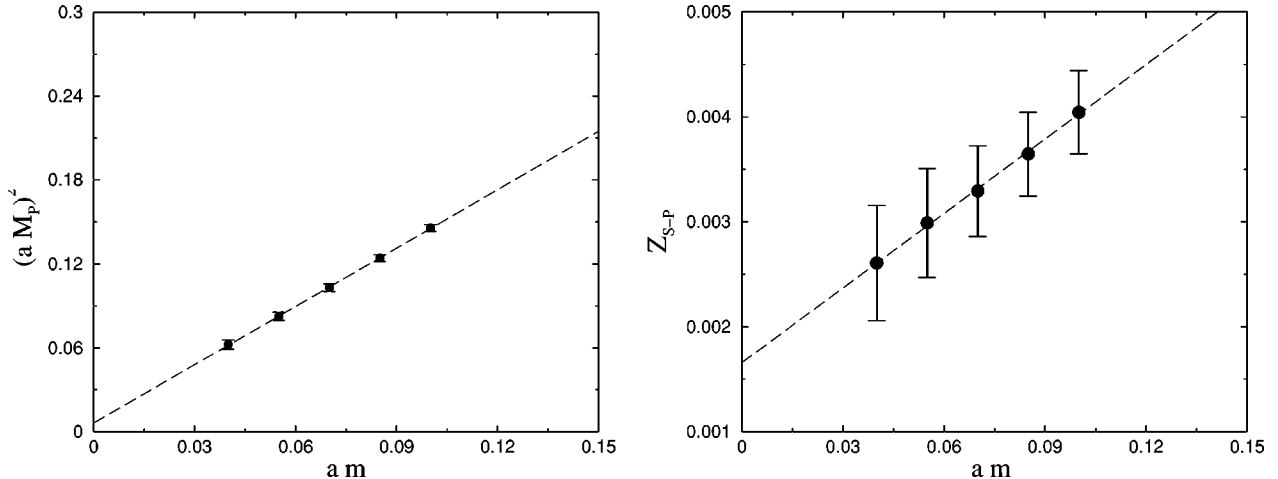

FIG. 3. $(aM_P)^2$ vs. am as obtained from $G_{S-P}(t)$ (left) and $G_{PP}(t)$ (right). The dashed lines represent the results of a linear fit.
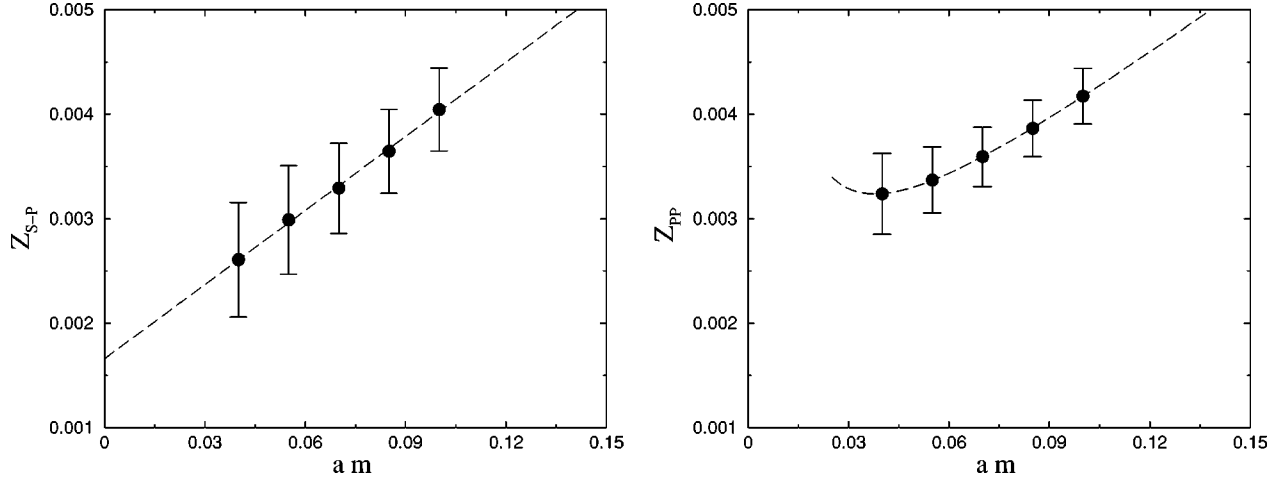
FIG. 4. Left: Z_{S-P} vs. (am); the dashed line represents the result of a linear fit. Right: Z_{PP} vs. (am); the dashed line represents a fit of the form of Eq. (41).

we obtain

$$\mathcal{A}_{PP} = 0.0014(3) \quad \mathcal{B}_{PP} = 0.024(2) \quad \mathcal{D}_{PP} = 0.000035(16).$$
(42)

Now the χ^2/d.o.f. of the fit turns out to be much smaller and the central values of intercepts and slope parameters for the fits of Z_{S-P} and Z_{PP} are much closer. The fact that the curvature shows up only in the results for Z_{PP} points to the fact that what we are seeing is the effect of the unsuppressed zero modes, and not of chiral logarithms which would affect both sets of results (and would most likely become noticeable at much smaller values of am). On account of the above, we will use $G_{S-P}(t)$ to derive our further results. It must also be said that some of the observables will be calculated directly at $m \simeq m_s/2$ (see below), and for these observables the difference between Z_{PP} and Z_{S-P} is irrelevant within our statistical error.
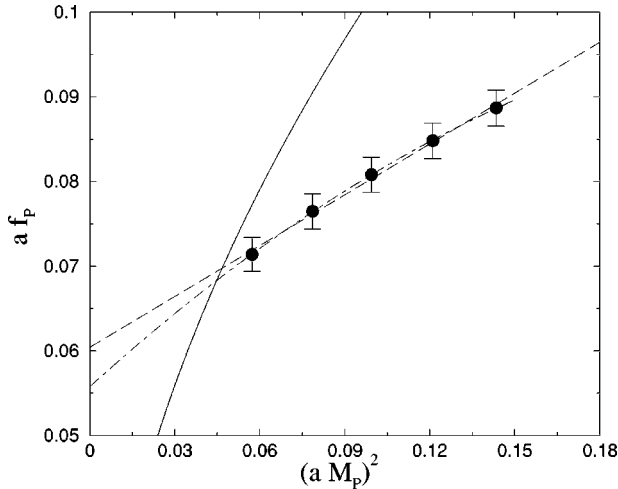

FIG. 5. The procedure used to derive af_K and aM_K. The dashed and dashed-dotted lines represent fits to our numerical results. The solid line represents the curve $(af_P) = C_{sl}(aM_P)$, where the coefficient $C_{sl} = f_K^{exp}/M_K^{exp}$.

The pseudoscalar decay constant is defined through Eq. (22) and we calculated its value directly from the parameters extracted from a cosh fit to $G_{S-P}(t)$:

$$af_P = 2(am) \frac{\sqrt{Z_{S-P}}}{(aM_P)^2}.$$
(43)

The values we obtained for af_P in correspondence to each simulated mass are reproduced in Table I [where we also reproduce the values derived from $G_{PP}(t)$] and are shown in Fig. 5. The dashed and the dot-dashed lines show the results of a linear and a quadratic fit in $(aM_P)^2$, respectively. The data slightly favors a quadratic fit, but our statistical accuracy is insufficient to rule out a linear fit as inconsistent with the data. It is interesting to observe, though, that we obtain $f_K/f_\pi \simeq 1.14$ and $\simeq 1.23$ from the linear and quadratic fits, respectively, with the results from the quadratic fit in much better agreement with the experimental value.

Starting from our values for M_P and f_P, we fix the lattice spacing a^{-1} and the physical meson masses by using the method of "lattice physical planes" [5]. This avoids recourse to a chiral extrapolation for observables where it is not really needed. In the plane $[af_P, (aM_P)^2]$, we plot our lattice data as well as the curve $(af_P) = C_{sl}(aM_P)$ (the solid line in Fig. 5), where the coefficient of proportionality C_{sl} (sl for strange-light) is fixed by the experimental value for the ratio f_K^{exp}/M_K^{exp}.[3] The point where the two lines meet determines af_K as well as aM_K. Since our statistical accuracy does not allow us to discriminate between a linear and quadratic fit to the data for af_P vs. $(aM_P)^2$, we just use the linear fit for the tiny extrapolation to the "kaon" point (see Fig. 5). Our results are

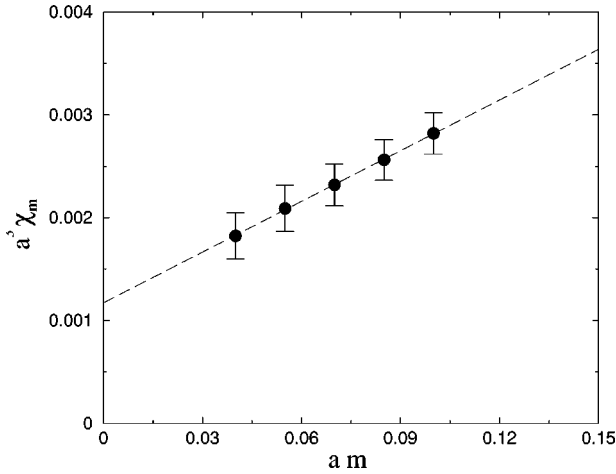$$aM_K = 0.216(8), \quad af_K = 0.0698(26).$$
(44)

FIG. 6. The data used to derive the chiral condensate from the GMOR relation.

(A quadratic fit produces a result which differs from the above by far less than the statistical errors.) To set the lattice spacing we compare the value of af_K with its experimental value and we get

$$a_{f_K}^{-1} = 2.29(9). \tag{45}$$

This is the value of the lattice spacing we will use throughout the paper. Again we stress that up to this stage we did not have to perform any chiral extrapolation, but derived all physical information, staying close to the region of quark masses used in the actual calculations.

From our data, we can also compute the chiral condensate by using the GMOR relation of Eq. (21). In Fig. 6 we show the quantity

$$a^3\chi_m = -(am)\frac{Z_{S-P}}{(aM_P)^2}, \tag{46}$$

as a function of the bare quark mass. The data exhibit very good linear behavior and a linear fit leads to

$$a^3\chi = -0.00117(27). \tag{47}$$

We performed also a quadratic fit to the data, obtaining a result consistent with zero for the coefficient of the quadratic term, but with an error twice as large in the intercept because of the additional degree of freedom. Therefore we conclude that we see no indication for a quadratic term in the fit within our statistical error.

The chiral condensate can also be computed directly from Eq. (16). However, away from the chiral limit, the r.h.s. of that equation contains power divergent terms [in a^{-1}, see Eq. (20)] and, in the quenched approximation, infrared divergent contributions (in m) due to the unsuppressed zero modes. Therefore quite a severe extrapolation from our simulated data is needed to determine its chiral value. One can take advantage, though, of a computational strategy similar to that used in Eq. (33). To remove the contribution due to unsuppressed zero modes, we subtract the scalar-

scalar correlation function from the r.h.s. of Eq. (17). From a quadratic fit in the quark mass we obtain

$$a^3\chi(a) = -0.00117(42) \tag{48}$$

which is in remarkable agreement with Eq. (47). Of course, the larger error is an indication of the difficulty of the extrapolation. Larger statistics and a careful treatment of the zero mode contributions would be needed to obtain more reliable and precise results by the direct method.

IV. PHYSICAL RESULTS

In this section we will use our lattice results to infer the renormalized values of the sum of the strange and average up-down quark masses and of the chiral condensate. To obtain our final values, we still need the value of the scalar renormalization constant $Z_S(\mu a)$, which we have computed non-perturbatively in the RI/MOM scheme following the approach proposed in [19]. The details of these calculations will be presented in a separate paper [28]. The result we obtained in the RI scheme is

$$Z_S^{\mathrm{RI}}(2 \ \mathrm{GeV}) = 1.24(5), \tag{49}$$

where the error is mainly systematics due to the chiral extrapolation and to the uncertainty in the value of the renormalization scale.[4] Judging from the comparison of the data at different renormalization scales with the logarithmic evolution predicted by the renormalization group equations at NNLO, the discretization errors appear to be well below the error in Eq. (49). The result in Eq. (49) differs by about 10% from the bare perturbation theory determination at one loop $[Z_S^{\mathrm{RI}}(2 \ \mathrm{GeV})]^{PT} = 1.11$ [25,26]. However if we use $\alpha_s^{\overline{\mathrm{MS}}}$ as an expansion parameter we obtain a result consistent within errors with Eq. (49). By using N^2LO continuum perturbation theory [35] with $N_f = 0$ and $\Lambda_{QCD} = 0.238(19)$ [12] to convert the result in Eq. (49) into the $\overline{\mathrm{MS}}$ scheme, we obtain

$$Z_S^{\overline{\mathrm{MS}}}(2 \ \mathrm{GeV}) = 1.41(6). \tag{50}$$

Had we used the experimental NNLO results from $\alpha_s(M_Z) = 0.118$, we would have obtained a value of the scalar renormalization constant $\sim 10\%$ higher than the one given above. The difference can be taken as an indication of the systematic error introduced by the quenched approximation. Therefore we will add this uncertainty in quadrature to our final estimate of the systematic error. Next-to-next-to-next-to-leading order NNNLO perturbative computations are available for the RI/$\overline{\mathrm{MS}}$ (modified minimal subtraction scheme) matching of the scalar renormalization constant [36], but the difference with the NNLO results is way below the error induced by the quenching ambiguity discussed above. If we had used the procedure proposed recently in Ref. [29] on our data, we would have obtained a value for $Z_S^{\overline{\mathrm{MS}}}(2 \ \mathrm{GeV})$

---

[4]We stress again that this number is obtained at $\beta = 6.0$ for $\rho = 1.4$ and $r = 1.0$.

which agrees within the errors with the one in Eq. (50), but with a central value $\simeq 5$–10% higher.

We finally combine this last result with the numbers presented in the previous section to obtain our main physical results. From the value of aM_K in Eq. (44) and from the lattice spacing in Eq. (45), we obtain, for the combination of bare quark masses,

$$m_s(a) + \hat{m}(a) = 149(9) \ \text{MeV}, \tag{51}$$

where the error is only statistical. Since our volume is fairly large, we expect our main sources of systematic errors to come from discretization effects and from the quenched approximation. For a rough estimate of the systematic error due to quenching approximation[5] we can use the results in Ref. [38]. From these one sees that, within the quenched approximation, the use of different observables to calculate the lattice spacing can produce differences in the results of $\sim 10\%$. Had we used r_0 [39] to fix our lattice spacing we would have obtained a number $\sim 7\%$ higher than the one in Eq. (51). Combining this fact with the results in [14], we would infer that discretization uncertainties are below 10%. In order to be conservative, we will take 15% as the estimate of our overall systematic error in the renormalized quark masses due to quenching and discretization effects. A more precise estimate of the systematic errors will need much more extensive simulations, which at present would be beyond our capability and the exploratory scope of this work. Combining the results in Eqs. (50) and (51) we obtain

$$(m_s + \hat{m})^{\text{RI}}(2 \ \text{GeV}) = 120 \pm 7 \pm 21 \ \text{MeV} \tag{52}$$

which represents one of the major results of this paper. By using Eqs. (1) and (50) the above translates to

$$m_s^{\overline{\text{MS}}}(2 \ \text{GeV}) = 102 \pm 6 \pm 18 \ \text{MeV}. \tag{53}$$

This result agrees very well with the current lattice world average [18].

Insofar as the value of the condensate is concerned, if we used the standard two-step approach, i.e., first measure the dimensionless condensate, see Eqs. (47) or (48), and then multiply it by the cubic power of the lattice spacing, the result would be affected by a very large systematic error due to the uncertainty in the determination of the lattice spacing in quenched simulations. Instead, we will use an alternative method [7]. We write the GMOR relation (23) for the renormalized condensate as follows

$$\chi(a) = -\tfrac{1}{4} f_\chi^2 \mathcal{B}_{M_P} a^{-1} \tag{54}$$

where $\mathcal{B}_{M_P}$ is defined in Eq. (36) and $f_\chi = 0.1282$ GeV is the "experimental" value, in physical units, of the pseudoscalar decay constant extrapolated to the chiral limit. While computing the condensate from the above formula relies on an

additional element of experimental information, it has several advantages. The most important is that, by expressing the condensate in terms of f_χ, we are left with only one power of the UV cutoff a^{-1}. Another advantage is that, if we assume that the relation between M_P and m stays substantially linear for a range of quark masses extending to $\sim m_s$ (and our numerical results validate this, see Fig. 3), then there is no need for an extrapolation to the chiral limit to evaluate $\mathcal{B}_{M_P}$. With this method we obtain

$$\langle \bar{\psi}\psi \rangle^{\text{RI}}(2 \ \text{GeV}) = -0.0167 \pm 0.0010 \pm 0.0029 \ \text{GeV}^3 \tag{55}$$

where the estimate of the systematic error has been made using the same criteria we used for estimate of the error in the quark mass. This is our best value for the chiral condensate. It is interesting to note that, if we had used the standard technique, starting from Eq. (47) and with the lattice spacing of Eq. (45), we would have obtained a result with a central value very close to the value in Eq. (55), but with a much higher systematic error.

Finally, from Eq. (55) and NLO matching, we get

$$\langle \bar{\psi}\psi \rangle^{\overline{\text{MS}}}(2 \ \text{GeV}) = -0.0190 \pm 0.0011 \pm 0.0033 \ \text{GeV}^3$$
$$= -[267 \pm 5 \pm 15 \ \text{MeV}]^3. \tag{56}$$

This result is in very good agreement with the result obtained by the authors of Refs. [37,29], while it is smaller than the result in Ref. [40], even if still compatible within errors. Our result is also compatible within errors with the number obtained few years ago in Ref. [7] with Wilson-type fermions. We expect, though, the systematics due to the discretization effects to be smaller ($\mathcal{O}(a^2)$) in the result reported in Eq. (56) than the error ($\mathcal{O}(a)$) which affects the determination in Ref. [7].

V. CONCLUSIONS

In the overlap regularization chiral symmetry is preserved at finite lattice spacing and finite volume, therefore there is no mixing among operators of different chirality. As a consequence no additive quark mass renormalization is required and no fine-tuned parameters are needed to compute $\mathcal{O}(a)$ improved masses and matrix elements. Our results have indeed produced a remarkable verification of "good chiral behavior" both in the axial Ward identity and in the pseudoscalar masses.

In this paper we presented the results of the first computation of $(m_s + \hat{m})$ with overlap fermions in the quenched approximation. To avoid uncertainties due to lattice perturbation theory, we computed the multiplicative renormalization constant $Z_S(\mu a)$ non-perturbatively in the RI/MOM scheme. Our main results have been summarized in the Introduction. While the systematics errors due to quenching are common to previous calculations, the other systematic errors (mostly discretization effects) are different than with other lattice regularizations and likely to be smaller, because of chiral symmetry. We also computed the chiral condensate

---

[5]First unquenched light quark mass computations (see Ref. [18] for details) give results $\sim 10\%$ lower with respect to the corresponding quenched determinations.

$\langle \bar{\psi}\psi \rangle$ from the GMOR relation and directly. Even if, given our statistical and systematic errors, the former method is more reliable, it is rewarding to notice that the two determinations are in good agreement.

The calculation of light quark masses uses many of the ingredients needed for a lattice calculation of weak matrix elements, although the latter is computationally more demanding. From this point of view, the very good agreement between our results for the quark masses and the current lattice world average bodes well for the use of the overlap formalism for matrix element calculations. Our investigation has been mostly of an exploratory nature. One would need to extend it to larger volumes and better statistics. One should also find a more direct way to isolate and account for the effects of the zero modes. Nevertheless, we believe that it gave a strong indication that the overlap formalism can be used effectively, with known algorithms and the present generation of computers, for large scale QCD

calculations, at least in the quenched approximation. Thus we would conclude that it represents a very promising nonperturbative regularization for solving long standing problems, such as the proof of the $\Delta I = 1/2$ rule and the calculation of ϵ'/ϵ, which would be hard to address with conventional regularizations.

ACKNOWLEDGMENTS

[1] J. Gasser and H. Leutwyler, Phys. Rep. **87**, 77 (1982).

[2] H. Leutwyler, Phys. Lett. B **378**, 313 (1996).

[3] C.R. Allton et al., Nucl. Phys. **B431**, 667 (1994).

[4] R. Gupta and T. Bhattacharya, Phys. Rev. D **55**, 7203 (1997).

[5] C.R. Allton, V. Gimenez, L. Giusti, and F. Rapuano, Nucl. Phys. **B489**, 427 (1997).

[6] B.J. Gough et al., Phys. Rev. Lett. **79**, 1622 (1997).

[7] V. Gimenez, L. Giusti, F. Rapuano, and M. Talevi, Nucl. Phys. **B540**, 472 (1999); **B531**, 429 (1998); L. Giusti, F. Rapuano, M. Talevi, and A. Vladikas, ibid. **B538**, 249 (1999).

[8] SESAM Collaboration, N. Eicker et al., Phys. Rev. D **59**, 014509 (1999).

[9] D. Becirevic et al., Phys. Lett. B **444**, 401 (1998).

[10] JLQCD Collaboration, S. Aoki et al., Phys. Rev. Lett. **82**, 4392 (1999).

[11] T. Blum, A. Soni, and M. Wingate, Phys. Rev. D **60**, 114507 (1999).

[12] S. Capitani, M. Luscher, R. Sommer, and H. Wittig, Nucl. Phys. **B544**, 669 (1999).

[13] M. Gockeler et al., Phys. Rev. D **62**, 054504 (2000).

[14] ALPHA Collaboration, J. Garden et al., Nucl. Phys. **B571**, 237 (2000).

[15] CP-PACS Collaboration, A. Ali Khan et al., Phys. Rev. Lett. **85**, 4674 (2000).

[16] S. Narison, Nucl. Phys. B (Proc. Suppl.) **86**, 242 (2000), and references therein.

[17] M. Davier et al., Nucl. Phys. B (Proc. Suppl.) **98**, 319 (2001), and references therein.

[18] V. Lubicz, Nucl. Phys. B (Proc. Suppl.) **94**, 116 (2001).

[19] G. Martinelli, C. Pittori, C.T. Sachrajda, M. Testa, and A. Vladikas, Nucl. Phys. **B445**, 81 (1995).

[20] R. Narayanan and H. Neuberger, Phys. Lett. B **302**, 62 (1993); Nucl. Phys. **B443**, 305 (1995); H. Neuberger, Phys. Lett. B **417**, 141 (1998); **427**, 353 (1998).

[21] P.H. Ginsparg and K.G. Wilson, Phys. Rev. D **25**, 2649 (1982).

[22] M. Lüscher, Phys. Lett. B **428**, 342 (1998).

[23] P. Hasenfratz, V. Laliena, and F. Niedermeyer, Phys. Lett. B **427**, 125 (1998).

[24] P. Hasenfratz, Nucl. Phys. **B525**, 401 (1998).

[25] C. Alexandrou, H. Panagopoulos, and E. Vicari, Nucl. Phys. **B571**, 257 (2000); C. Alexandrou, E. Follana, H. Panagopoulos, and E. Vicari, ibid. **B580**, 394 (2000).

[26] S. Capitani and L. Giusti, Phys. Rev. D **62**, 114506 (2000); **64**, 014506 (2001).

[27] K. Jansen et al., Phys. Lett. B **372**, 275 (1996); M. Lüscher, S. Sint, R. Sommer, and H. Wittig, Nucl. Phys. **B491**, 344 (1997).

[28] L. Giusti, C. Hoelbling, and C. Rebbi (in preparation).

[29] P. Hernández, K. Jansen, L. Lellouch, and H. Wittig, J. High Energy Phys. **07**, 018 (2001).

[30] We retrieved the first 54 gauge configurations OSU_Q60a produced by G. Kilcup, D. Pekurovsky, and L. Venkataraman, Nucl. Phys. B (Proc. Suppl.) **53**, 345 (1997), from the repository at the ''Gauge Connection'' (http://qcd.nersc.gov/).

[31] H. Neuberger, Phys. Rev. Lett. **81**, 4060 (1998); R.G. Edwards, U.M. Heller, and R. Narayanan, Nucl. Phys. **B540**, 457 (1999).

[32] R.G. Edwards, U.M. Heller, and R. Narayanan, Phys. Rev. D **59**, 094510 (1999).

[33] S.J. Dong, F.X. Lee, K.F. Liu, and J.B. Zhang, Phys. Rev. Lett. **85**, 5051 (2000).

[34] T. Blum et al., Phys. Rev. D (to be published), hep-lat/0007038.

[35] T. van Ritbergen, J.A.M. Vermaseren, and S.A. Larin, Phys. Lett. B **400**, 379 (1997); J.A.M. Vermaseren, S.A. Larin, and T. van Ritbergen, ibid. **405**, 327 (1997); K.G. Chetyrkin, ibid. **404**, 161 (1997); E. Franco and V. Lubicz, Nucl. Phys. **B531**, 641 (1998).

[36] K.G. Chetyrkin and A. Retey, Nucl. Phys. **B583**, 3 (2000).

[37] P. Hernández, K. Jansen, and L. Lellouch, Phys. Lett. B **469**, 198 (1999).

[38] CP-PACS-Collaboration, S. Aoki et al., Phys. Rev. D **60**, 114508 (1999).

[39] ALPHA Collaboration, M. Guagnelli, R. Sommer, and H. Wittig, Nucl. Phys. **B535**, 389 (1998).

[40] MILC Collaboration, T. DeGrand, Phys. Rev. D **63**, 034503 (2001); ibid. (to be published), hep-lat/0107014.